

Critical interface of an ionic Ising mixture

Craig L. Caylor, Bruce M. Law, and Piyal Senanayake

Department of Physics, Kansas State University, Manhattan, Kansas 66506-2601

Vladimir L. Kuzmin

Department of Higher Mathematics, Institute of Trade and Economics, 198018 St. Petersburg, Russia

Vadim P. Romanov

Department of Physics, St. Petersburg State University, 198904 Petrodvoretz, St. Petersburg, Russia

Simone Wiegand

Institut für Physikalische und Anorganische Chemie, Universität Bremen, 28334 Bremen, Germany

(Received 5 May 1997)

Ellipsometric measurements at the liquid-liquid interface of a critical ionic Ising mixture yield a decrease in the ellipticity $\bar{\rho}$ as the reduced temperature t is decreased (for $t > 0.002$) in contrast to a $t^{\beta-\nu}$ power-law divergence found for nonionic Ising mixtures. From this surprising result we infer the existence of an anisotropic interface. A model of such an interface is used to calculate theoretical $\bar{\rho}$ data, which capture some of the characteristics of the experimental results. [S1063-651X(97)08510-3]

PACS number(s): 68.10.-m, 64.60.Fr, 61.20.Qg, 68.35.Rh

I. INTRODUCTION

It is widely known that nonionic fluids or fluid mixtures [1] that exhibit second-order phase transitions belong to the Ising universality class and display Ising critical exponents ($\beta=0.33$, $\nu=0.63$, and $\gamma=1.24$) that describe the thermodynamic behavior of the fluid as it approaches the critical point (in agreement with renormalization-group theory). This agreement between theory and experiment does not necessarily hold for *ionic* fluids or fluid mixtures near second-order phase transitions. Systems have been discovered that exhibit mean-field critical exponents [2–6] ($\beta=0.5$, $\nu=0.5$, and $\gamma=1.0$) even very close to the critical temperature (T_c) and yet other critical ionic systems have been discovered that exhibit Ising behavior close to T_c [7–9]. Much of the earlier work on critical ionic systems has extracted the critical behavior from systems that exhibit very high critical temperatures (~ 1000 K) where it is difficult to obtain good temperature stability and good temperature resolution [10].

A clearer experimental picture of the relevant parameters that govern the fluid properties of critical ionic systems at small reduced temperatures $t=|T-T_c|/T_c$ only started to emerge after Pitzer and co-workers [2–4] and Weingärtner *et al.* [11] started examining large organic salts in solution where the critical temperatures are around room temperature. Though the details regarding these systems' behaviors are far from clear at this time, there appear to be essentially two types of critical ionic mixtures, which have been called Coulombic mixtures and solvophobic (or hydrophobic) mixtures. The type of critical behavior exhibited by these mixtures is thought to depend upon the range of the interaction between the ions of the dissociated salt. For an attractive interparticle potential characterized by $V(r) \approx -(1/r)^p$, where r is the separation distance, the critical exponents begin to depart from Ising values for $p < 4.97$, where the critical exponents γ , ν , and η become p dependent [12]. Below $p=4.5$, γ as-

sumes the classical value of 1, but ν and η still remain p dependent; for $p < 3$ no theoretical predictions exist. For a Coulombic interaction between dissociated salt ions $p=1$ and hence no definitive theoretical predictions are available. The presence of a solvent significantly complicates the situation. Not only is the “bare” Coulombic interaction screened by a cloud of counterions around each ion, according to the Debye-Hückel theory [13] where the screening length $\kappa^{-1} \sim (\rho/\epsilon)^{1/2}$, ρ is the ion density, and ϵ is the static dielectric constant of the solvent, but also for polar solvents solvation shells can form around each ion [14] where the solvent molecules in the immediate vicinity of the ion are orientationally ordered. The solvent medium between ions is now structured; the interaction between ions in such structured media is not well understood at this time. Nevertheless, a simple model that captures some of the observed experimental trends classifies Coulombic mixtures as dissociated salts in solvents of low static dielectric constant. These mixtures are hypothesized to exhibit mean-field behavior where the phase separation is believed to be driven primarily by electrostatic effects. In contrast, solvophobic mixtures are classified as dissociated salts in solvents of high static dielectric constant. These mixtures exhibit normal Ising behavior where the phase separation is driven primarily by solvophobic effects rather than electrostatic effects. For intermediate values of the solvent static dielectric constant, crossovers from mean-field to Ising behavior have been observed in a number of systems [15–18] as the critical temperature is approached. There are exceptions to this oversimplified Coulombic-solvophobic picture where the structure of the solvent and/or ions appears to play an important role. Levelt Sengers, Harvey, and Wiegand [19] provide a concise summary of the current experimental situation.

The presence of minute amounts of impurities can also complicate the situation. Preliminary results [20] for the system triethyl-*n*-hexylammonium triethyl-*n*-hexylboride

($N_{2226}B_{2226}$) in the solvent diphenyl ether [$(C_6H_5)_2O$] suggest that under certain conditions the gross behavior of a system can be changed from mean field to Ising (or perhaps vice versa) by the presence of impurities, although no systematic investigation of this effect has yet been attempted. In nonionic critical fluids it is well known and has been well documented [21] that the presence of minute impurities can change the critical temperature and under certain conditions renormalize the critical exponents [21]. This latter effect, called Fisher renormalization [22], does not appear to be the explanation of the impurity effect observed in this critical ionic system [20]. Mysterious impurity effects in a nonionic critical mixture, which cannot be explained by Fisher renormalization, have been noted by other investigators [23]. For a variety of theoretical reasons it is believed that all systems should ultimately exhibit Ising behavior sufficiently close to T_c [24,25]; however, it is not understood why some systems exhibit mean-field behavior even exceptionally close to T_c .

As far as we are aware, the interfacial behavior of critical ionic systems has never been studied previously either experimentally or theoretically. In this paper we study the behavior of the critical liquid-liquid interface of a critical mixture of $N_{2226}B_{2226}$ in the solvent diphenyl ether (henceforth denoted NBD) using the surface-sensitive technique of Brewster angle ellipsometry. This technique measures the ellipticity $\bar{\rho} = \text{Im}(r_p/r_s)|_{\theta_B}$, where r_p and r_s are the reflection amplitudes in the p and s polarization directions and θ_B is the Brewster angle. The variation of the ellipticity with the reduced temperature (t) provides information about the interfacial structure.

Previously it had been found that the system NBD is a Coulombic mixture that exhibits mean-field behavior. The mean-field behavior has been documented from measurements of the coexistence curve by Singh and Pitzer [3,4] and turbidity by Zhang *et al.* [6]. More recent turbidity measurements by Wiegand *et al.* [20] on a different sample of NBD appear to show Ising behavior. Our sample was prepared by Wiegand and Briggs and also exhibits Ising-like bulk behavior (determined via turbidity measurements) in agreement with [20]. We review the bulk measurements taken on the sample NBD in more detail in Sec. III. Regardless of this controversy concerning the bulk behavior of NBD, our sample definitely exhibits Ising behavior in the bulk. We therefore expect Ising behavior at the critical liquid-liquid interface.

For non-ionic critical fluids or fluid mixtures (which exhibit Ising behavior in the bulk) it has been well documented on pure fluids [26], binary mixtures [27], and polymer solutions [28] using the technique of ellipsometry that $\bar{\rho} \sim t^{\beta-\nu}$ at the critical interface; $\bar{\rho}$ diverges as one approaches T_c . This divergence is independent of the specific form assumed for the interfacial profile and just originates from the thermal behavior of the two bulk coexisting phases ($\psi = \psi_0 t^\beta$) and the bulk correlation length ($\xi = \xi_0 t^{-\nu}$).

Surprisingly we find that for our critical ionic Ising mixture $\bar{\rho}$ exhibits a minimum at a reduced temperature of $t \sim 0.002$. The only explanation that seems capable of explaining this unusual temperature dependence of $\bar{\rho}$ is the presence of additional orientational order at the critical interface, which is absent in the adjacent bulk liquid phases.

In these systems there is a prevalence of neutral ion pairs in solution [29], each with a large effective dipole moment. An appropriate analog for an ionic mixture composed of neutral ion pairs would therefore appear to be a dipolar fluid. We have therefore compared our experimental results of the critical interfacial behavior of our Ising ionic mixture with the theoretical results of Frodl and Dietrich [30], who predict additional orientational order at the critical interface of dipolar fluids.

This paper is set up as follows. Details concerning the sample preparation of our mixture are provided in Sec. II. In Sec. III we review the experimental results obtained thus far for the bulk properties of the system NBD. In Sec. IV we describe the contributions to the ellipticity $\bar{\rho}$ for both a locally isotropic interface and a locally anisotropic interface, while in Sec. V the experimental data for the critical interface of NBD are presented. The Frodl-Dietrich model of the orientational order that occurs at the critical dipolar fluid interface is described in Sec. VI together with both a simpler analytic model that incorporates all of the essential features of the Frodl-Dietrich calculation and an example of the model's results for the ellipticity. Finally, we discuss the experimental results in light of our model calculations in Sec. VII.

II. SAMPLE PREPARATION

Wiegand *et al.* [20] prepared a large number of samples of NBD, including our sample, in order to measure various properties of this system. $N_{2226}B_{2226}$ was synthesized by Strem Chem with a reported purity of better than 98%. No unreacted components were present; the major remaining impurity was hexane used for washing the salt. A better-than-average 99+ % batch of diphenyl ether was purchased from Aldrich Chemical Company and degassed by a repeated freeze-pump-thaw cycle before use. $N_{2226}B_{2226}$ decomposes in the presence of air; therefore, all samples were prepared in a dry box flushed with 99.9995% dry argon gas to prevent contamination of the salt. The critical concentration was determined to be $x_c = 4.9 \pm 0.1$ mole % of salt. For this composition the two coexisting phases had equal volumes 5 mK below the phase separation temperature.

The sample cell for examining the critical liquid-liquid interface was made from a well-annealed Pyrex cylinder with approximate length and diameter of 7.5 and 2.5 cm, respectively. The interior of the cell was cleaned with a glass etching solution for 60 s (5 vol % HF, 35 vol % HNO_3 , and 60 vol % H_2O [31]), rinsed well in distilled deionized water, and dried at a high temperature before it was filled with the critical solution. After repeated freeze-pump-thaw cycles the cell was backfilled with high-purity dry argon gas before tipping off. The backfilling with argon gas, to slightly less than 1 atm, minimized any strain birefringence due to pressure differentials across the glass. At no time did the solution come into contact with air or water vapor. When used in the ellipsometer the sample cell had its long axis horizontal; the critical liquid-liquid interface is situated in the middle of the sample cell in this geometry. The critical temperature was initially 36.345 °C, but drifted down by 0.335 °C over a period of 6 months.

III. BULK CRITICAL IONIC PROPERTIES OF NBD

The bulk critical properties of critical ionic systems have been extensively reviewed elsewhere [10,19,32,33]. In this section we summarize the bulk properties of NBD, which is the system of interest in this paper.

The coexistence curve of a binary liquid mixture can be described in simple scaling by an equation of the form

$$\psi = |v - v_c| = \psi_0 t^\beta, \quad (1)$$

where ψ is the order parameter, ψ_0 is a nonuniversal amplitude, v is a composition (e.g., volume fraction), and v_c is the critical composition. In practice, however, it is often necessary to account for various corrections to simple scaling. This is often done in a Wegner expansion

$$\psi = \psi_0 t^\beta (1 + \psi_1 t^\Delta + \psi_2 t^{2\Delta} + \dots), \quad (2)$$

where Δ is usually set to 0.5 and terms beyond ψ_1 are rarely needed.

Singh and Pitzer measured the coexistence curve for NBD [3]. Their measurements, which approached to within approximately one degree of the critical temperature, were well described by a coexistence curve with a mean field $\beta=0.5$. A later set of measurements [4] approached closer to T_c and an exponent of $\beta=0.476$ was reported in the case of simple scaling. When the data were fitted to Eq. (2) with β fixed at either its Ising ($\beta=0.326$ was used) or classical value, both values of β were found to be consistent with the measurements, though with an anomalously large value of ψ_1 for the Ising case. The mean-field behavior for the system NBD has been confirmed by Zhang *et al.* [6] from turbidity measurements where a value of $\gamma=1.01$ was obtained; the effects of correction terms to simple scaling were not considered.

It was expected that our sample of NBD would show mean-field behavior in the bulk, as was previously found for this system. However, turbidity measurements by Wiegand *et al.* [20] on other samples prepared under identical conditions have supported Ising exponents for ν and γ . For a beam with incident intensity I_0 and transmitted intensity I , the turbidity τ is given by

$$\tau = -\frac{1}{d} \ln(I/I_0), \quad (3)$$

where d is the sample path length. Turbidity measurements allow experimental access to the critical exponents ν and γ because for the critical part of the turbidity τ_c ,

$$\tau_c \approx f(\alpha) t^{-\gamma}, \quad (4)$$

where $\alpha = (2\pi\xi/\lambda)^2 \sim t^{-2\nu}$ and the Ornstein-Zernike correction factor $f(\alpha)$ is given by

$$f(\alpha) = (2\alpha^2 + 2\alpha + 1)\alpha^{-3} \ln(1 + 2\alpha) - 2(1 + \alpha)\alpha^{-2}. \quad (5)$$

In the analysis $\nu = \gamma/2$ is assumed. This relationship is exact for mean-field critical exponents and approximately correct for Ising critical exponents. Additionally, there is a noncritical background contribution to the turbidity τ_{back} , which can be significant.

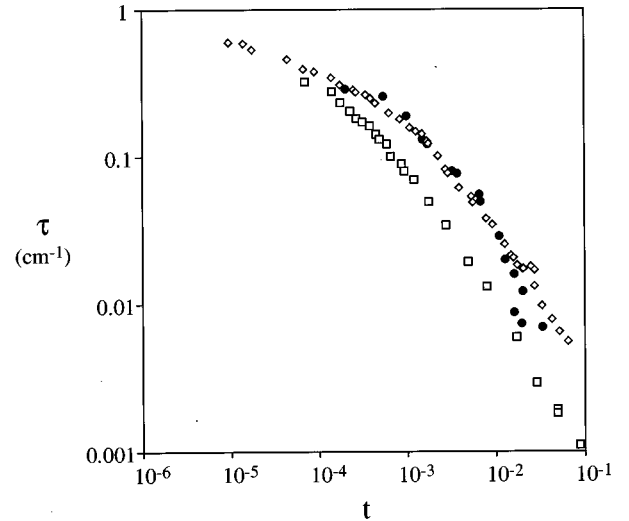


FIG. 1. Turbidity measurements on NBD. Open squares represent mean-field measurements from Zhang *et al.* [6], open diamonds are the Ising measurements from Wiegand *et al.* [20], and closed circles depict measurements from our sample, demonstrating that our system exhibits Ising exponents in the bulk.

Turbidity measurements by Wiegand *et al.* [20] were made on different critical samples of $N_{2226}B_{2226}$ in diphenyl ether. The resulting data exhibited Ising-like behavior with $\nu \sim 0.62$; however, a full analysis is still in progress. This Ising-like behavior is quite at odds with the classical result reported earlier by Zhang *et al.* [6]. Wiegand *et al.* [20] therefore carefully re-examined the original turbidity data of Zhang *et al.* and reconfirmed that these data indeed exhibited mean-field behavior; however, they noted that unpublished results of Zhang on a small 1-cm-long cell (which was not ideal for measuring turbidity accurately because of its short length) exhibited large drifts in the turbidity in the first 2 months after loading where the turbidity increased by a factor of ~ 3 over this period of time. The original Zhang *et al.* turbidity measurements [6] were collected in the first 3 weeks after loading; unfortunately this sample could not be re-examined due to its premature breakage and therefore it is not known whether or not this cell exhibited similar time-dependent drifts.

Our cell was prepared by Wiegand *et al.* and therefore we expected it to exhibit Ising behavior. In Fig. 1 we compare turbidity measurements on our sample cell with the measurements of Wiegand *et al.* [20] and Zhang *et al.* [6]. We indeed find very good agreement with the measurements of Wiegand *et al.* We do not understand why these samples have shown such markedly different bulk behavior compared to that found by previous studies.

It is not known what role impurities play in this controversy, namely, whether a minute amount of some impurity could convert a mean-field mixture to an Ising mixture or vice versa. For the system NBD Singh and Pitzer [3] have noted that 1.2 wt. % of water increased T_c by 40 °C, while 1% of methylene chloride decreased T_c by 20 °C. No appreciable change in the shape of the coexistence curve was noticed.

IV. SURFACE CONTRIBUTIONS TO THE ELLIPTICITY

The interface between the two liquid phases of a phase-separated binary liquid mixture has a thickness that diverges as the correlation length. For an Ising system the intrinsic order parameter profile $\psi(z)$ varies between the bulk values of the upper and lower phases according to the well-known Fisk-Widom profile [34]

$$\psi(z) = v(z) - v_c = \frac{1}{2}(v_b - v_a)f(z/2\xi), \quad (6)$$

where

$$f(Y) = \tanh(Y) \sqrt{\frac{2}{3 - \tanh^2(Y)}}, \quad (7)$$

v_b (v_a) is the bulk concentration of salt in the lower (upper) phase described by Eq. (1), and z is the distance measured perpendicular to the interface from the plane defined by $v(z) = v_c$. We have chosen the z axis so that z is negative in the upper salt-rich a phase and positive in the lower salt-poor b phase. For horizontal length scales greater than the bulk correlation length the interface is roughened by the presence of thermally generated capillary waves [35].

Phase-modulated ellipsometry [36] is a particularly effective and convenient method for probing surface structure and has been used for many years to probe the interfacial structure in a large variety of systems [37]. For the intrinsic profile, in the absence of any surface fluctuations, the coefficient of ellipticity $\bar{\rho} = \text{Im}(r_p/r_s)|_{\theta_B}$ measured at the Brewster angle, where $\text{Re}(r_p/r_s) = 0$, is expressed to first order in interfacial thickness by the Drude equation [38]

$$\bar{\rho}_{\text{int}} = \frac{\pi}{\lambda} \frac{\sqrt{\varepsilon_a + \varepsilon_b}}{\varepsilon_a - \varepsilon_b} \int \frac{[\varepsilon(z) - \varepsilon_a][\varepsilon(z) - \varepsilon_b]}{\varepsilon(z)} dz, \quad (8)$$

which holds for thin profiles (compared to the optical wavelength $\lambda = 633$ nm) and isotropic media, where ε_a and ε_b are the optical dielectric constants of the two bulk phases. Here $\varepsilon(z)$ is the dielectric profile through the interface, which can be calculated from Eq. (6) using the Clausius-Mossotti relation applied to mixtures [39]

$$F(\varepsilon(z)) = v(z)F(\varepsilon_a) + [1 - v(z)]F(\varepsilon_b), \quad (9a)$$

where $v(z)$ is taken as the volume fraction and

$$F(x) = \frac{x - 1}{x + 2}, \quad (9b)$$

assuming that there is no volume change on mixing. Marvin and Toigo [40] have shown that in the Drude region the intrinsic and capillary wave contributions to $\bar{\rho}$ are additive

$$\bar{\rho} = \bar{\rho}_{\text{int}} + \bar{\rho}_{\text{cw}}. \quad (10)$$

Kuzmin and Romanov [41] determined an expression, accurate to first order in $\Delta\varepsilon = \varepsilon_a - \varepsilon_b$, for the capillary wave component for a *locally isotropic* interface

$$\bar{\rho}_{\text{cw}} = \sqrt{2} \frac{\pi}{\lambda} \xi \Delta n \eta_R, \quad (11)$$

where $\Delta n = n_a - n_b$ is the refractive index difference between the two bulk phases. In this equation

$$\eta_R = \frac{3}{32\pi R} \int_{-\infty}^{\infty} \frac{d\kappa}{2\pi} |\varphi(\kappa)|^2 \ln[1 + (2a_0/\kappa)^2], \quad (12)$$

$R = 0.128$, $a_0 = 0.748$, and $\varphi(\kappa)$ is the inverse Fourier transform of the derivative of $f(Y)$ [Eq. (7)], given by

$$\varphi(\kappa) = \int_{-\infty}^{\infty} dY \frac{df(Y)}{dY} \exp(-i\kappa Y). \quad (13)$$

Equations (11) and (12) are expected to be valid at the critical interface where $\Delta\varepsilon \sim t^\beta \rightarrow 0$ as $t \rightarrow 0$, but these equations may not be very accurate at a noncritical liquid-vapor interface where $\Delta\varepsilon$ is large. Equations (8) and (12) are valid only for locally isotropic interfaces where $\varepsilon_{\parallel}(z) = \varepsilon_{\perp}(z) = \varepsilon(z)$ and $\varepsilon_{\parallel}(z), \varepsilon_{\perp}(z)$ are, respectively, the variations in the optical dielectric constants parallel and perpendicular to the interface. For locally anisotropic surface layers where $\varepsilon_{\parallel}(z) \neq \varepsilon_{\perp}(z)$, $\bar{\rho}_{\text{int}}$ and η_R , given in Eqs. (8) and (12), must be replaced by [36,42]

$$\bar{\rho}_{\text{int}} = \frac{\pi}{\lambda} \frac{\sqrt{\varepsilon_a + \varepsilon_b}}{\varepsilon_a - \varepsilon_b} \int \varepsilon_{\parallel}(z) + \frac{\varepsilon_a \varepsilon_b}{\varepsilon_{\perp}(z)} - (\varepsilon_a + \varepsilon_b) dz \quad (14)$$

and [43]

$$\eta_R = \frac{1}{32\pi R} \int_{-\infty}^{\infty} \frac{d\kappa}{2\pi} [|\phi_{\parallel}(\kappa)|^2 + 2|\phi_{\perp}(\kappa)|^2] \times \ln[1 + (2a_0/\kappa)^2]. \quad (15)$$

The functions $\varphi_{\parallel}(\kappa)$ and $\varphi_{\perp}(\kappa)$ are the analogs of $\varphi(\kappa)$ [Eq. (13)] parallel and perpendicular to the interface.

V. EXPERIMENTAL RESULTS

For nonionic critical binary liquid mixtures (which are known to exhibit Ising behavior in the bulk) one can readily show [26–28,41] that Eqs. (8) and (11) for the critical interface reduce to

$$\bar{\rho} = \bar{\rho}_{\text{int}} + \bar{\rho}_{\text{cw}} \sim t^{\beta-\nu}. \quad (16)$$

This result holds for any locally isotropic dielectric profile $\varepsilon(z) = \varepsilon_c + \Delta\varepsilon X(z/\xi)$, independently of the precise form of the universal surface scaling function $X(z/\xi)$. Schmidt and co-workers have made the most detailed experimental study of the critical interface for ordinary binary liquid mixtures and found excellent agreement with the expected $t^{\beta-\nu}$ divergence for binary liquid mixtures [27], polymer solutions [28], and pure fluids [26]. In fact, quantitative agreement is found between all the experimental systems and the theoretical results given in Eqs. (6)–(13) with no adjustable parameters [41].

In order to test the accuracy of our experimental setup, a few ellipsometric measurements were taken on the liquid-liquid interface of a critical sample of carbon disulfide and methanol. In Fig. 2 the results of these measurements (open

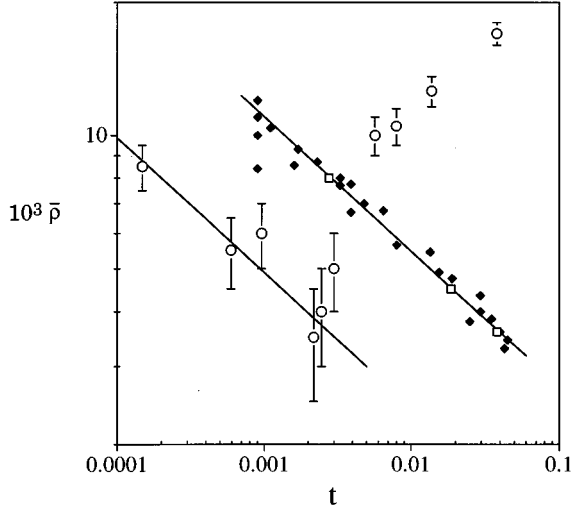


FIG. 2. Schmidt's ellipsometric measurements on the critical interface of $\text{CS}_2+\text{CH}_3\text{OH}$ [27] are shown as filled diamonds. The open squares are our measurements for $\text{CS}_2+\text{CH}_3\text{OH}$, in excellent agreement with those of Schmidt. Our measurements on the system NBD are shown as open circles with error bars of $\pm 1 \times 10^{-3}$. The solid lines possess a slope of -0.3 corresponding to $\bar{\rho} \sim t^{\beta-\nu} \sim t^{-0.3}$, which is valid for locally isotropic surfaces where $\epsilon_{\parallel}(z) = \epsilon_{\perp}(z)$.

squares) are compared with Schmidt's data (solid diamonds) for the same system [27], and agreement with Schmidt's data is noted.

For the critical ionic mixture NBD the sample was heated well above the critical temperature into the one-phase region before each measurement and shaken well to ensure that the sample was homogeneous before quenching the sample into the two-phase region. This procedure precluded the system from remaining in a metastable two-phase state, which might happen if a temperature quench were made from one two-phase state to another two-phase state. After phase separation had occurred, the Brewster angle was found and $\bar{\rho}$ was monitored continuously until it stabilized. The sample temperature was monitored at both ends of the sample cell. We were careful to keep the temperature gradient across the sample cell to less than 2 mK/cm. The temperature of the sample was taken as the average of the two end-point temperatures and was stable within ± 2 mK. Data taken on the sample of NBD were very unstable, with the value of $\bar{\rho}$ fluctuating dramatically at times. Singh and Pitzer [4] had previously noted that it takes this system a very long time to phase separate, perhaps because of the very small differences in density between the two phases and the high viscosity. When $\bar{\rho}$ had stabilized into the neighborhood of a particular value for more than 24 h, we took that value as the actual value with suitably large error bars of $\pm 1 \times 10^{-3}$.

The data collected as a function of reduced temperature for NBD are shown in Fig. 2 (open circles). The ellipticity $\bar{\rho}$ for NBD obviously does not exhibit a $t^{\beta-\nu}$ temperature dependence. In fact, a decrease in $\bar{\rho}$ is found for decreasing t far from T_c ($t > 0.002$), rather than a divergence as observed in all other Ising mixtures studied to date. This decrease crosses over to a divergence for smaller t ($t < 0.002$) with approximate $t^{\beta-\nu}$ behavior in this region. The fact that $\bar{\rho}$

does not scale with $t^{\beta-\nu}$ far from T_c implies that the interface is *not* locally isotropic. The equations that describe a locally anisotropic interface [Eqs. (14) and (15)] do not automatically lead to the prediction that $\bar{\rho} \sim t^{\beta-\nu}$, except in the isotropic limit. In the next section we consider a model that qualitatively explains the observed behavior for $\bar{\rho}$.

VI. SURFACE ORIENTATIONAL ORDER

The existence of an anisotropic interface can be readily explained for an ionic system. It is known that many of the ions in solution pair up to form neutral dipoles [29]; this pairing is an essential ingredient in the modified Debye-Hückel-Bjerrum theory of Fisher and Levin [44], which calculated the critical temperature and critical concentration for the restricted primitive model. Furthermore, calculations by Frodl and Dietrich (FD) [30] provide strong evidence for orientational ordering of dipolar molecules near the critical interface of a phase-separated dipolar fluid. Our model calculations suggest that for strong dipoles with moderately anisotropic refractive index ellipsoids, this orientational ordering alters significantly the temperature dependence of $\bar{\rho}$.

Each dipole in the solution has a refractive index tensor that can be represented by an ellipsoid with semimajor axes n_1 , n_2 , and n_3 , where we choose the n_1 axis to point in the same direction as the dipole moment and $n_2 = n_3$ because $N_{2226}B_{2226}$ is a prolate spheroid. Then the parallel (ϵ_{\parallel}^d) and perpendicular (ϵ_{\perp}^d) components of a dipole's dielectric constant are given as a function of the dipole's orientation θ relative to the z axis of the sample by

$$\epsilon_{\perp}^d(\theta) = \frac{\epsilon_1 \epsilon_2}{\epsilon_2 \cos^2 \theta + \epsilon_1 \sin^2 \theta}, \quad (17)$$

$$\epsilon_{\parallel}^d(\theta) = \epsilon_2 \sqrt{\frac{\epsilon_1}{\epsilon_1 \cos^2 \theta + \epsilon_2 \sin^2 \theta}}, \quad (18)$$

where $\epsilon_j = n_j^2$, $j = 1, 2$. Throughout the remainder of this paper a superscript d refers to a property of the dipole. For randomly oriented dipoles, integrating $\epsilon_{\parallel}^d(\theta)$ and $\epsilon_{\perp}^d(\theta)$ over θ yields the expected result $\epsilon_{\parallel}^d = \epsilon_{\perp}^d = \bar{\epsilon}^d$.

However, orientational ordering of the dipoles introduces a weighting factor that causes ϵ_{\parallel}^d and ϵ_{\perp}^d to be different. FD [30] composed a model of the liquid-vapor interface for a Stockmayer fluid of dipole moment m in which the number density \hat{n} of particles with an orientation θ relative to the z axis is given by

$$\hat{n}(z, \theta) = n(z) \alpha(z, \theta) \quad (19)$$

where n is the total number density and α determines the angular distribution. The dependence of α on θ is expressed in terms of Legendre polynomials

$$\alpha(z, \theta) = \frac{1}{2} + \frac{3 \cos^2 \theta - 1}{2} \alpha_2(z) + \dots \quad (20)$$

Preferential orientation is then expressed solely by the parameter $\alpha_2(z)$.

From their simulation data, FD obtained the result that

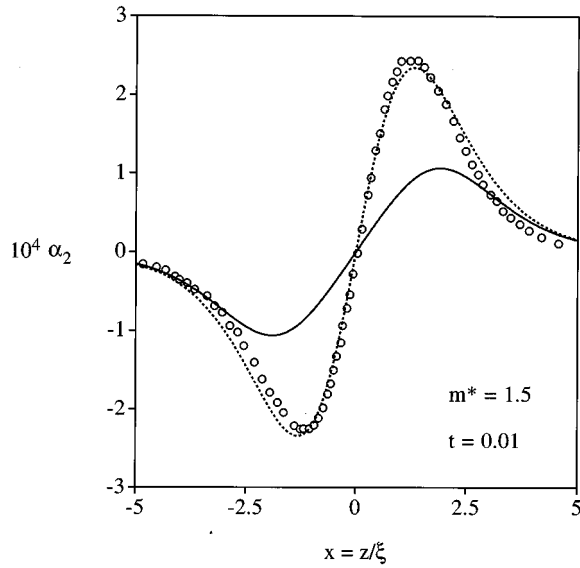


FIG. 3. Comparison of our model for α_2 [Eq. (22)] with the numerical calculations of Frodl and Dietrich [30]. The mean-field result for our model is shown as a dotted line, while the result for the Fisk-Widom profile is shown as a solid line. Open circles represent data from Fig. 9 in Ref. [30].

$$\alpha_2(z) \sim m^* t^{\beta+2\nu} Y(z/\xi), \quad (21a)$$

where

$$m^* = \frac{m}{\sqrt{\sigma^3 u_0}} \quad (21b)$$

is the reduced dipole moment, σ is an average hard-sphere diameter for the dipole, u_0 is the Lennard-Jones interaction well depth, and the function $Y(z/\xi)$ scales with the correlation length. The numerical techniques used by FD to generate the functional form of $\alpha_2(z)$ were impractical for our use, so following a suggestion of Sluckin [45], which is correct in the limit $m \rightarrow 0$, we have assumed the following ansatz in all our calculations:

$$\alpha_2(z, t) \approx \frac{D \xi_0^2 m^* t^{\beta+2\nu}}{\psi_0} \frac{d^2 \psi(z)}{dz^2}, \quad (22)$$

where $\psi(z)$ is the Fisk-Widom order parameter profile through the critical interface [Eq. (6)]. This form for α_2 recovers all of the essential features determined in [30]. The width of our ansatz for α_2 scales with ξ , it has qualitatively the correct shape as a function of the distance z through the interface, and it recovers the expected $t^{\beta+2\nu}$ temperature dependence. The parameter D is a dimensionless constant whose value was chosen to obtain the correct absolute magnitude for α_2 at the peak value. For $m^* = 1.5$ at a reduced temperature of $t = 0.01$, FD [30] obtained a peak value of $\alpha_2(\max) = 2.34 \times 10^{-4}$; for agreement at the peak we require that $D = 0.2402$. FD's calculations assume the mean-field result for the profile through the interface, $\psi(z) \approx \tanh(z/2\xi)$. In Fig. 3, for $m^* = 1.5$ and $t = 0.01$, we compare our ansatz for the mean-field profile (dotted line) with the calculated profile of FD (open circles) [30]. The agreement between the

two models is quite remarkable. Our ansatz for the Fisk-Widom profile is also shown (solid line); we have assumed that D remains unchanged for this profile. We note that calculations by different groups [46], using differing theoretical methods at the liquid-vapor interface (far from T_c), produced forms for $\alpha_2(z)$ that qualitatively agree with the features in [30], but differ quantitatively in the precise shape of α_2 . We therefore believe that the ansatz in Eq. (22) is a sufficiently accurate representation of the essential features of the theoretical models. The presence of orientational order at the liquid-vapor surface far from any critical points has also been well documented experimentally in many different systems [47].

From Eqs. (17), (18), (20), and (22) the angle-averaged z variation of the dipole's dielectric constant parallel [$\varepsilon_{\parallel}^d(z)$] and perpendicular [$\varepsilon_{\perp}^d(z)$] to the interface can be calculated from

$$\varepsilon_j^d(z) = \int_0^{\pi} \varepsilon_j^d(\theta) \alpha(z, \theta) \sin \theta \, d\theta, \quad j = \parallel, \perp. \quad (23)$$

The parallel [$\varepsilon_{\parallel}(z)$] and perpendicular [$\varepsilon_{\perp}(z)$] dielectric constant through the interface for the salt solution can be calculated from a Clausius-Mossotti relation

$$F(\varepsilon_j(z)) = v(z) F(\varepsilon_j^d(z)) + [1 - v(z)] F(\varepsilon_s), \quad j = \parallel, \perp, \quad (24)$$

where $\varepsilon_j^d(z)$ is obtained from Eq. (23), ε_s (≈ 2.5) is the solvent optical dielectric constant, $v(z)$ is the local volume fraction of dipoles obtained from Eq. (6) if the volume fraction difference is taken as the order parameter, and $F(x)$ is given in Eq. (9b). In Eq. (6) $v_b - v_a$ is determined from the bulk coexistence curve [Eq. (1)] where for NBD the critical volume fraction of $N_{2226}B_{2226}$ is taken to be $v_c = 0.135$ [3], while ψ_0 (≈ 0.261) was estimated from the coexistence curve measurements in [4] assuming an Ising exponent of $\beta = 0.328$. The correlation length amplitude in the two-phase region, ξ_{0-} , has been assumed to be 8.0 \AA [20].

The solution dielectric profiles $\varepsilon_{\parallel}(z)$ and $\varepsilon_{\perp}(z)$ [Eq. (24)] are used to determine $\bar{\rho}_{\text{int}}$ and η_R for an anisotropic surface layer [Eqs. (14) and (15)] from which the total ellipticity $\bar{\rho}$ can be calculated from Eqs. (10) and (11) [48]. The values of ε_1 and ε_2 used in Eqs. (17) and (18) are not known for the dipoles formed in solution; however, the average value

$$\bar{\varepsilon}^d = \frac{1}{2} \int_0^{\pi} \varepsilon_{\perp}^d(\theta) \sin \theta \, d\theta \sim 1.9 \quad (25)$$

can be determined from the critical value of the refractive index [4] using the Clausius-Mossotti relationship. We have therefore considered the behavior of $\bar{\rho}$ as a function of ε_1 where the appropriate value of ε_2 is calculated from Eq. (25).

The reduced dipole moment m^* [Eq. (21b)] is not well known for $N_{2226}B_{2226}$ dissolved in diphenyl ether principally because the separation distance L between the ions that enters the dipole moment $m = qL$ is not well known. The minimum reasonable separation is set by the ionic radius of the nitrogen and boron ions N^{+1} and B^{-1} , which can be estimated from [49] to give $L_{\min} \approx 1.75 \text{ \AA}$, while the maximum

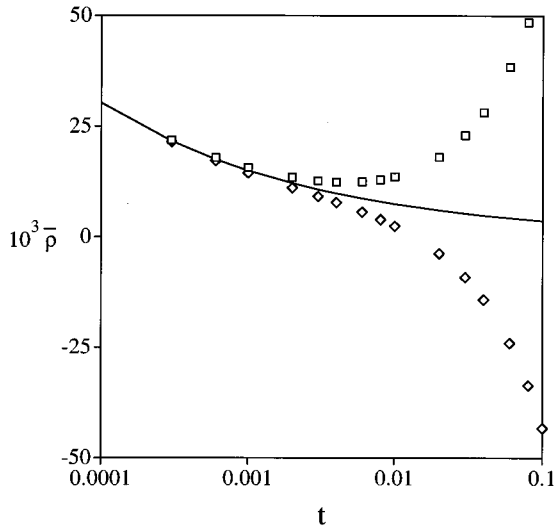


FIG. 4. Calculations of the variation in the ellipticity for an anisotropic critical interface. For a reduced dipole moment of $m^* = 6.39$, open squares are the results for $\epsilon_1 = 1.5 < \epsilon_2 = 2.148$, while open diamonds are the results for $\epsilon_1 = 2.3 > \epsilon_2 = 1.732$. The solid line depicts the isotropic result.

separation will certainly be less than the effective diameter of the ion in solution, $L_{\max} < 7 \text{ \AA}$ [32]. From these upper and lower bounds for L we find that $8.4 \text{ D} < m < 34 \text{ D}$ and therefore $5000 \text{ D}^4 < m^4 < 10^6 \text{ D}^4$. The depth of the interaction well u_0 between two neutral dipoles can be estimated by comparing the attractive potential of FD [30], $4u_0(\sigma/r)^6$, with the corresponding expression for the total van der Waals interaction that decays proportionally to r^{-6} [50]. There is a large variation in the value m^* that can assume. We have therefore treated it as an adjustable parameter in our calculation in order to see how its variation influences $\bar{\rho}$.

A representative sample of the numerical calculations is shown in Fig. 4 for a fixed value of $m^* = 6.39$. The solid line represents the result in the absence of any surface anisotropy ($\alpha_2 = 0$) where $\bar{\rho} = \bar{\rho}_{\text{int}} + \bar{\rho}_{\text{cw}}$ [Eqs. (10), (11), (14), and (15)] diverges proportionally to $t^{\beta-\nu}$. The symbols are for an anisotropic surface where the open squares are for $\epsilon_1 = 1.5 < \epsilon_2 = 2.148$, while the open diamonds are for $\epsilon_1 = 2.3 > \epsilon_2 = 1.732$. We note first that $\bar{\rho}$ approaches the isotropic result as $t \rightarrow 0$, as is expected because in this limit $\alpha_2 \rightarrow 0$. For $\epsilon_1 > \epsilon_2$, $\bar{\rho}$ decreases below the isotropic case and can become negative for sufficiently large t . For this type of interface $\bar{\rho}$ is a monotonically increasing function with decreasing t . For $\epsilon_1 < \epsilon_2$, $\bar{\rho}$ increases above the isotropic case and can exhibit a minimum in $\bar{\rho}$ at a particular reduced temperature. Increasing the difference between ϵ_1 and ϵ_2 , i.e., making the dielectric ellipsoid more anisotropic, causes $\bar{\rho}$ to diverge more sharply away from the isotropic case as might be expected. Also increasing the magnitude of m^* similarly causes $\bar{\rho}$ to diverge more sharply away from the isotropic case because the larger reduced dipole moment causes stronger alignment of the dipoles at the interface.

The divergence of $\bar{\rho}$ from the isotropic case is dominated by the behavior of the intrinsic profile contributions [Eq. (14)]. In order to highlight the variation of the capillary wave

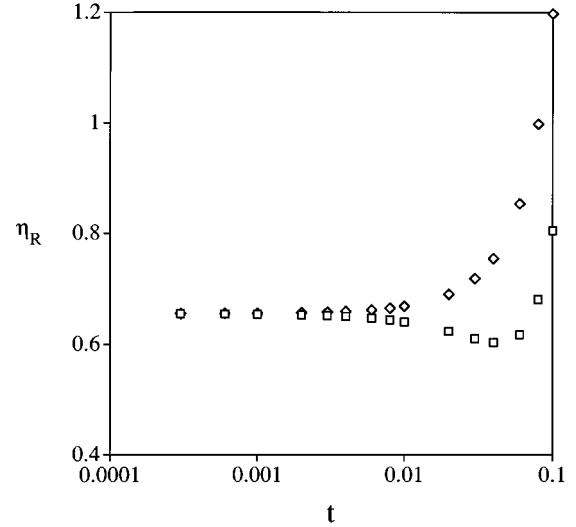


FIG. 5. Calculated values of η_R for an anisotropic critical interface, from which the capillary wave contribution to the ellipticity can be determined. For a reduced dipole moment of $m^* = 6.39$, we depict the results for $\epsilon_1 = 1.5 < \epsilon_2 = 2.148$ (open squares) and for $\epsilon_1 = 2.3 > \epsilon_2 = 1.732$ (open diamonds). The isotropic case results in a constant value $\eta_R = 0.655$.

contributions, which are hidden in Fig. 4, we present the results of η_R [Eq. (15)] in Fig. 5, where the symbols are for the same values of m^* , ϵ_1 , and ϵ_2 as in Fig. 4. As $t \rightarrow 0$, we regain the expected result that η_R is a constant. However, Kuzmin and Romanov [41] obtain the value $\eta_R = 0.77$, whereas our calculations result in a somewhat lower value of $\eta_R = 0.655$ for the isotropic limit. The explanation for this discrepancy is the different choices of order parameter made in the two calculations. Kuzmin and Romanov assume that the local dielectric constant difference $\epsilon(z) - \epsilon_c$ varies through the interface as the Fisk-Widom profile. Our calculations assume that the local volume fraction difference $v(z) - v_c$ follows the Fisk-Widom profile. Essentially, Kuzmin and Romanov choose $\epsilon(z) - \epsilon_c$ as the local order parameter, while the anisotropic nature of $\epsilon(z)$ in our calculations renders that choice impossible for our use [51].

VII. CONCLUSION

In this paper we have examined the critical liquid-liquid interface of the organic salt $\text{N}_{2226}\text{B}_{2226}$ in the solvent diphenyl ether (NBD) using the experimental technique of Brewster angle ellipsometry, which measures the ellipticity $\bar{\rho}$ of the interface. Our critical mixture exhibited Ising exponents in the bulk and therefore we expected to observe Ising behavior at the interface where $\bar{\rho}$ diverges proportionally to $t^{\beta-\nu}$ with decreasing t . Surprisingly, we found that the ellipticity initially decreased with decreasing t and then began to diverge for t below $\sim 2 \times 10^{-3}$; $\bar{\rho}$ apparently exhibits a minimum at around $t \sim 2 \times 10^{-3}$.

It is rather well known that in these critical ionic salt solutions ions readily form neutral ion pairs with large effective dipole moments. We have therefore modeled this system as a critical dipolar fluid; for such a fluid Frodl and Dietrich [30] predict that the critical interface will exhibit additional

orientational order that will be absent in the bulk. We have used an appropriate analytic model [Eq. (22)] that incorporates all the essential features of the Frodl-Dietrich calculations to estimate the effect of orientational order on the ellipticity of a critical interface. Qualitative agreement between this model and experiment would be obtained provided $\varepsilon_1 < \varepsilon_2$; both the model and the experiment exhibit a minimum in $\bar{\rho}$ at similar reduced temperatures and exhibit a $\sim t^{\beta-\nu}$ divergence at still smaller reduced temperatures. The model calculations for this system (Fig. 4) are a factor of ~ 3 larger than the experimental measurements (Fig. 2). This discrepancy could be caused by the values we have assumed for either the amplitude of the coexistence curve ψ_0 or the amplitude of the correlation length ξ_{0-} [52].

It is difficult to obtain even qualitative estimates of ε_1 and ε_2 required in the calculation. Although the dielectric anisotropy can be calculated for very simple molecules [53], the calculation becomes progressively more difficult for larger molecules [54]. The calculation of the dielectric anisotropy appears to be particularly difficult for this case because the polarizability of ions can only be calculated for simple ions [55], and this polarizability is undoubtedly influenced by the interionic separation L , which is an unknown quantity for this system. An experimental measurement of ε_1 and ε_2 for neutral ionic dipoles also appears to be difficult. Typically for nondissociated molecules, ε_1 , ε_2 , and ε_3 are determined from the average refractive index, a Kerr constant measurement, and a depolarized light scattering measurement where the latter two measurements are conducted either in the gaseous phase or in a nonpolar solvent in the limit of infinite dilution for the polar solute of interest [56,57]. A Kerr constant measurement [57], which requires high electric fields, is problematic for ionic solutions because of the presence of ions, while a depolarized light scattering measurement can only determine $(\varepsilon_1 - \varepsilon_2)^2$ [56] and the sign of $\varepsilon_1 - \varepsilon_2$ is not accessible. Also in the limit of infinite dilution, neutral ionic dipoles become less common, while free ions in solution become more prevalent [29].

Most molecules have $\varepsilon_1 > \varepsilon_2$ [53], namely, the optical dielectric constant is larger along the dipole axis compared to perpendicular to the dipole axis. It is therefore a little unusual that we require that $\varepsilon_2 > \varepsilon_1$ in order that we obtain qualitative agreement with our experimental results. A possible explanation for this requirement is that the electron lone pairs on the oxygen of the diphenyl ether interact with the dissociated ions of $\text{N}_{2226}\text{B}_{2226}$ causing orientational alignment of the diphenyl ether molecules in the immediate vicinity of the ions and it is the neutral ion pairs plus the surrounding solvation shell of diphenyl ether molecules that are aligning at the interface. A method for testing such a hypothesis would be examining the critical liquid-liquid interface of $\text{N}_{2226}\text{B}_{2226}$ in a nonpolar solvent; for such a system one would expect that $\varepsilon_1 > \varepsilon_2$ and therefore the $\bar{\rho}$ curve should follow the trend indicated by the open diamonds in Fig. 4. Schröder [58] has suggested alternative explanations for $\varepsilon_2 > \varepsilon_1$ for neutral ion pairs, such as those formed by $\text{N}_{2226}\text{B}_{2226}$ in solution, where the molecular orientation of the two hexyl chains relative to the effective dipole moment maybe important. A molecularly based experimental study would be required to distinguish between these various possibilities.

For critical ionic mixtures, one should not expect precise quantitative agreement between the model of Frodl and Dietrich [30] and experimental results. This is because the proportion of free ions to neutral ion pairs in solution may change as a function of reduced temperature. Also no account has been taken of larger neutral and singly charged clusters that are expected to be present [29]. (In our calculation we have assumed that all ions occur as neutral ion pairs.) The model used by Frodl and Dietrich also deviates somewhat from reality (although we expect it to capture many of the essential physical features) because the model assumes spherically shaped molecules of diameter σ , that possess a large dipole moment m . Real molecules with large dipole moments usually are very asymmetric in shape.

A further limitation of this study is that we have assumed that the two bulk phases only differ in the concentration of NB molecules present, as described by the coexistence curve [Eq. (1)]. It is not known whether or not the molecular configuration of the NB molecules is identical in the two phases.

We are currently using the theoretical model developed in this paper to calculate the magnitude of the surface anisotropy effect on $\bar{\rho}$ in normal dipolar systems where ε_1 , ε_2 , and m are known. Schmidt and co-workers [26–28] never observed any anisotropy effects in their studies of nonionic critical fluids; however, the systems that they studied typically had small dipole moments ($m < 2$ D) and an insufficiently large anisotropy in the refractive index ellipsoid to produce noticeable effects on $\bar{\rho}$.

An additional limitation of FD's model is that it is strictly valid only for small m^* . For large m^* other density-functional methods are available [59]. Kuzmin and Romanov [43] have qualitatively considered this regime of large m^* ; their results suggest that $\bar{\rho}$ can be considered to be the sum of two terms

$$\bar{\rho} = \bar{\rho}^{(\text{Is})} + \bar{\rho}^{(\text{Es})} \quad (26)$$

where the universal Ising-like term $\bar{\rho}^{(\text{Is})} \sim t^{\beta-\nu}$ dominates close to T_c , while the nonuniversal electrostatic term $\bar{\rho}^{(\text{Es})} \sim t^\beta$ dominates far from T_c . The electrostatic term is non-universal because the particular form it assumes is dependent upon the form of the interaction. Such a competition between two terms, with varying reduced temperature dependences, can also qualitatively explain the experimental data [43]. Further theoretical work is required to unify these theoretical results at small and large m^* before a complete theoretical picture can emerge.

ACKNOWLEDGMENTS

We wish to thank Dr. Benjamin Lee for fruitful discussions on the bulk properties of critical ionic systems, Dr. Matthew Briggs for assistance with filling the sample cell, Dr. Johanna Levelt Sengers for extensive advice throughout the course of this work, Ashish Mukhopadhyay for assistance with the ellipsometric measurements, and Professor S. Dietrich for useful correspondence. This work was supported by the National Science Foundation through Grant No. DMR-9500827. S.W. received a research grant from the Alexander von Humboldt Foundation in support of this work.

- [1] H. E. Stanley, *Introduction to Phase Transitions and Critical Phenomena* (Oxford, New York, 1971); A. Kumar, H. R. Krishnamurthy, and E. S. R. Gopal, *Phys. Rep.* **98**, 57 (1983); J. V. Sengers and J. M. H. Levelt Sengers, *Annu. Rev. Phys. Chem.* **37**, 189 (1986).
- [2] K. S. Pitzer, M. C. P. de Lima, and D. R. Schreiber, *J. Phys. Chem.* **89**, 1854 (1985).
- [3] R. R. Singh and K. S. Pitzer, *J. Am. Chem. Soc.* **110**, 8723 (1988).
- [4] R. R. Singh and K. S. Pitzer, *J. Chem. Phys.* **92**, 6775 (1990).
- [5] H. Weingärtner, S. Wiegand, and W. Schröer, *J. Chem. Phys.* **96**, 848 (1992).
- [6] K. C. Zhang, M. E. Briggs, R. W. Gammon, and J. M. H. Levelt Sengers, *J. Chem. Phys.* **97**, 8692 (1992).
- [7] M. L. Japas and J. M. H. Levelt Sengers, *J. Phys. Chem.* **94**, 5361 (1990).
- [8] W. Schröer, S. Wiegand, and H. Weingärtner, *Ber. Bunsenges. Phys. Chem.* **97**, 975 (1993).
- [9] S. Wiegand, M. Kleemeier, J.-M. Schroder, W. Schröer, and H. Weingärtner, *Int. J. Thermophys.* **15**, 1045 (1994).
- [10] Much of the earlier work on critical ionic systems is well reviewed in J. M. H. Levelt Sengers and J. A. Given, *Mol. Phys.* **80**, 899 (1993).
- [11] H. Weingärtner, T. Merkel, U. Maurer, J. Conzen, H. Glasbrenner, and S. Käshammer, *Ber. Bunsenges. Phys. Chem.* **95**, 1579 (1991).
- [12] G. Stell, *Phys. Rev. B* **1**, 2265 (1970); **8**, 1271 (1970); M. E. Fisher, S. Ma, and B. G. Nickel, *Phys. Rev. Lett.* **29**, 917 (1972); R. F. Kayser and H. J. Raveche, *Phys. Rev. A* **29**, 1013 (1984).
- [13] P. Debye and E. Hückel, *Phys. Z.* **24**, 185 (1923); **24**, 305 (1923).
- [14] J. N. Israelachvili, *Intermolecular and Surface Forces*, 2nd ed. (Academic, London, 1992).
- [15] P. Chieux and M. J. Sienko, *J. Chem. Phys.* **53**, 566 (1970); F. Leclercq, P. Damay, and P. Chieux, *Z. Phys. Chem. (Munich)* **156**, 183 (1988).
- [16] T. Narayanan and K. S. Pitzer, *J. Phys. Chem.* **98**, 9170 (1994); T. Narayanan and K. S. Pitzer, *Phys. Rev. Lett.* **73**, 3002 (1994).
- [17] T. Narayanan and K. S. Pitzer, *J. Chem. Phys.* **102**, 8118 (1995).
- [18] M. Kleemeier, S. Wiegand, T. Derr, V. Weiss, W. Schröer, and H. Weingärtner, *Ber. Bunsenges. Phys. Chem.* **100**, 27 (1996).
- [19] J. M. H. Levelt Sengers, A. H. Harvey, and S. Wiegand, in *Equations of State*, edited by J. V. Sengers and H. J. White, Jr. (Blackwell, Cambridge, 1996).
- [20] S. Wiegand, J. M. H. Levelt Sengers, K. J. Zhang, M. E. Briggs, and R. W. Gammon, *J. Chem. Phys.* **106**, 2777 (1997).
- [21] J. L. Tveekrem and D. T. Jacobs, *Phys. Rev. A* **27**, 2773 (1983).
- [22] M. E. Fisher and P. E. Scesney, *Phys. Rev. A* **2**, 825 (1970).
- [23] M. Corti and V. Degiorgio, *Phys. Rev. Lett.* **55**, 2005 (1985); G. Dietler and D. S. Cannell, *ibid.* **60**, 1852 (1988).
- [24] G. Stell, *Phys. Rev. A* **45**, 7628 (1992); *J. Stat. Phys.* **78**, 197 (1995).
- [25] B. P. Lee and M. E. Fisher, *Bull. Am. Phys. Soc.* **41**, 377 (1996).
- [26] J. W. Schmidt and M. R. Moldover, *J. Chem. Phys.* **99**, 582 (1993).
- [27] J. W. Schmidt, *Phys. Rev. A* **38**, 567 (1988).
- [28] D. G. Miles, Jr. and J. W. Schmidt, *J. Chem. Phys.* **92**, 3881 (1990).
- [29] N. Bjerrum, K. Dan. Vidensk. Selsk. Mat. Fys. Medd. **7**, 1 (1926); M. J. Gillan, *Mol. Phys.* **49**, 421 (1983); K. S. Pitzer and D. R. Schreiber, *ibid.* **60**, 1067 (1987).
- [30] P. Frodl and S. Dietrich, *Phys. Rev. E* **45**, 7330 (1992); **48**, 3741 (1993).
- [31] L. Holland, *The Properties of Glass Surfaces* (Chapman and Hall, London, 1964).
- [32] K. S. Pitzer, *Acc. Chem. Res.* **23**, 333 (1990).
- [33] M. E. Fisher, *J. Stat. Phys.* **75**, 1 (1994).
- [34] S. Fisk and B. Widom, *J. Chem. Phys.* **50**, 3219 (1969).
- [35] F. P. Buff, R. A. Lovett, and F. H. Stillinger, *Phys. Rev. Lett.* **15**, 621 (1965).
- [36] D. Beaglehole, *Physica B & C (Amsterdam)* **100**, 163 (1980).
- [37] D. Beaglehole, in *Fluid Interfacial Phenomena*, edited by C. A. Croxton (Wiley, New York, 1986).
- [38] P. K. L. Drude, *The Theory of Optics* (Dover, New York, 1959), p. 292.
- [39] R. F. Kayser, *Phys. Rev. B* **34**, 3254 (1986).
- [40] A. M. Marvin and F. Toigo, *Phys. Rev. A* **26**, 2927 (1982).
- [41] V. L. Kuzmin and V. P. Romanov, *Phys. Rev. E* **49**, 2949 (1994).
- [42] J. Lekner, *Mol. Phys.* **49**, 1385 (1983).
- [43] V. L. Kuzmin and V. P. Romanov (private communication).
- [44] M. E. Fisher and Y. Levin, *Phys. Rev. Lett.* **71**, 3826 (1993); M. E. Fisher, Y. Levin, and X. Li, *J. Chem. Phys.* **101**, 2273 (1994).
- [45] T. J. Sluckin, *Mol. Phys.* **47**, 267 (1982); **43**, 817 (1981).
- [46] E. Chacon, P. Tarazona, and G. Navascues, *J. Chem. Phys.* **79**, 4426 (1983); J. Eggebrecht, K. E. Gubbins, and S. M. Thompson, *ibid.* **86**, 2286 (1987); **86**, 2299 (1987).
- [47] M. C. Goh, J. M. Hicks, K. Kemnitz, G. R. Pinto, K. Bhattacharyya, K. B. Eisenthal, and T. F. Heinz, *J. Phys. Chem.* **92**, 5074 (1988); S. G. Grubb, M. W. Kim, Th. Rasing, and Y. R. Shen, *Langmuir* **4**, 452 (1988); R. Superfine, J. Y. Huang, and Y. R. Shen, *Phys. Rev. Lett.* **66**, 1066 (1991).
- [48] In order to calculate Eq. (15) we require forms for $df_{\parallel}(Y)/dY$ and $df_{\perp}(Y)/dY$ in Eq. (13). We assume that (see Ref. [41]) $df_i/dY = (4\xi/\Delta\varepsilon)d\varepsilon_i(z)/dz$, $i = \parallel, \perp$, where $\Delta\varepsilon = \varepsilon_a - \varepsilon_b$ is the difference in the optical dielectric constants of the two phases.
- [49] *Handbook of Chemistry and Physics*, 66th ed., edited by R. C. Weast, M. J. Astle, and W. H. Beyer (CRC, Boca Raton, FL, 1985), p. F-164. The ionic radius of N^{+1} is 0.25 Å, while the ionic radius of B^{-1} has been estimated to be ~ 1.5 Å from the ionic radii of O^{-1} and F^{-1} , which are other elements in period 2 of the Periodic Table.
- [50] Reference [14], Eq. (6.35), p. 101. This equation is strictly valid only for $r \gg \sigma$; however, it is probably a reasonable initial estimate for u_0 .
- [51] It is not obvious from Eqs. (12) and (13) for the capillary wave contributions how the difference in order parameters enters the calculation. In Ref. [41], $\varphi(\kappa)$ in Eq. (13) is given by the inverse Fourier transform of $(4\xi/\Delta\varepsilon)d\varepsilon/dY$. This quantity is equal to df/dY when $\varepsilon(z)$ is the local order parameter.
- [52] In Ref. [6], a value for ξ_{0-} is determined that is a factor of 2 smaller than in Ref. [20].
- [53] K. G. Denbigh, *Trans. Faraday Soc.* **36**, 936 (1940); J. O. Hirschfelder, C. F. Curtiss, and R. B. Bird, *Molecular Theory of Gases and Liquids* (Wiley, New York, 1954), p. 947.

- [54] G. M. Aval, R. L. Rowell, and J. J. Barrett, *J. Chem. Phys.* **57**, 3104 (1972); T. Keyes and B. M. Ladanyi, *Adv. Chem. Phys.* **56**, 411 (1984).
- [55] G. D. Mahan and K. R. Subbaswamy, *Local Density Theory of Polarizability* (Plenum, New York, 1990), Chap. 4.
- [56] I. L. Fabelinskii, *Molecular Scattering of Light* (Plenum, New York, 1968).
- [57] C. G. Le Fevre and R. J. W. Le Fevre, *Rev. Pure Appl. Chem.* **5**, 261 (1955).
- [58] W. Schröer (private communication).
- [59] G. Stell, G. N. Patey, and G. S. Hoye, *Adv. Chem. Phys.* **48**, 185 (1980); V. L. Kuzmin, *Phys. Rep.* **123**, 365 (1985).